Soft Matter

PAPER

View Article Online
View Journal | View Issue

Cite this: *Soft Matter*, 2020, **16**, 4655

Active noise experienced by a passive particle trapped in an active bath

Simin Ye,†[ab] Peng Liu,†[ab] Fangfu Ye,*[abcd] Ke Chen*[abc] and Mingcheng Yang *[ab]

We study the properties of active noise experienced by a passive particle harmonically trapped in an active bath. The active bath is either explicitly simulated by an ensemble of active Brownian particles or abstractly represented by an active colored noise in theory. Assuming the equivalence of the two descriptions of the active bath, the active noise in the simulation system, which is directly extracted by fitting theoretical predictions to simulation measurements, is shown to depend on the constraint suffered by the passive tracer. This scenario is in significant contrast to the case of thermal noise that is independent of external trap potentials. The constraint dependence of active noise arises from the fact that the persistent force on the passive particle from the active bath can be influenced by the particle relaxation dynamics. Moreover, due to the interplay between the active collisions and particle relaxation dynamics, the effective temperature of the passive tracer quantified as the ratio of fluctuation to dissipation increases as the constraint strengthens, while the average potential and kinetic energies of the passive particle both decrease.

Received 2nd January 2020,
Accepted 20th April 2020

DOI: 10.1039/d0sm00006j

rsc.li/soft-matter-journal

1 Introduction

Active colloids consist of mesoscale self-propelled units that are able to locally convert stored or ambient energy into their persistent locomotion.[1–3] Prominent examples include colonies of bacteria[4–6] and synthetic microswimmers.[7–13] Due to being intrinsically out of equilibrium, active colloidal suspensions can serve as an active bath that can profoundly impact the structure and dynamics of immersed passive objects. For instance, an active bath can greatly deform flexible macromolecules,[14–19] or give rise to unusual effective interactions between passive objects[20–22] or unexpected self-assemblies.[23–27] Moreover, an active bath can dramatically enhance the diffusion of passive tracers by orders of magnitude compared to thermal cases,[28,29] and can drive a directed motion of asymmetric objects.[6,30–32] These phenomena are fundamentally different from equilibrium thermal baths. Despite their important differences, the generalization of important physical concepts and relations (such as temperature, pressure, depletion force, equation of state or fluctuation relation) from thermal to active bath has recently attracted considerable attention.[33–41]

Neglecting the internal degrees of freedom, the effect of an equilibrium thermal bath on a tracer particle can be well described by thermal stochastic force and friction,[42] which are connected by the fluctuation dissipation theorem. For a given system, the thermal noise on a tracer particle is uniquely determined by the properties of the thermal bath, independent of external conditions such as external constraints, forces or boundaries. Similarly, one may characterize an active bath by introducing a time-correlated active noise that takes into account the persistent collisions between the passive tracers and active microswimmers.[28,43] Such active noise no longer follows the fluctuation–dissipation relation, thus breaking the detailed balance. This minimal model has recently been successfully applied to a harmonically confined passive colloidal particle in an active bath,[43–49] which constitutes a paradigm to study nonequilibrium statistical physics.[50–52] The active noise, although artificially imposed in theories,[46–49] can be directly extracted from colloidal experiments or simulations. It is implicitly assumed that the active noise is an intrinsic feature of the active bath, similar to the thermal noise in equilibrium, and is completely determined by the active swimmers, the passive tracers and their interactions.[43–49] Recent studies, however, suggest that active pressure depends on the details of external boundary walls[53] and active depletion force drastically changes with external constraints.[54] These observations raise the fundamental questions of whether and how external conditions influence the active noise.

[a] *Beijing National Laboratory for Condensed Matter Physics and Institute of Physics, Chinese Academy of Sciences, Beijing 100190, China. E-mail: fye@iphy.ac.cn, mcyang@iphy.ac.cn, kechen@iphy.ac.cn*
[b] *School of Physical Sciences, University of Chinese Academy of Sciences, Beijing 100049, China*
[c] *Songshan Lake Materials Laboratory, Dongguan, Guangdong 523808, China*
[d] *Wenzhou Institute, University of Chinese Academy of Sciences, Wenzhou, Zhejiang 325001, China*
† These authors contributed equally to this work.

In this paper, we study the dynamics of a passive particle suspended in an active bath, trapped by harmonic potentials of various stiffness, using computer simulations and theoretical analyses. In simulations, the active bath is modelled by an ensemble of active Brownian particles (ABPs); and in theory, the active bath is described by an active noise. By fitting the theoretical prediction to the simulation measurement, we find that the extracted active noise, both its magnitude and correlation time, sensitively depends on the constraint experienced by the passive particle, in contrast to its thermal counterpart. An intuitive explanation for this constraint dependence of active noise is that the external trapping influences the intensity of collisions between the tracer and active particles. The theoretical model with a constraint-dependent active noise quantitatively reproduces the mean potential energy of the tracer particle measured in simulations. Furthermore, we show that three widely used effective temperatures (separately quantified as the ratio of fluctuation to dissipation, and the average potential and kinetic energies of the passive particle) all change significantly with the external constraint, but in different manners. Our results demonstrate that the active noise experienced by a confined passive tracer cannot be treated as an intrinsic physical quantity of the active bath, and a single constant effective temperature is not sufficient to describe the tracer behaviors.

2 Simulation and theory

Simulation

The simulation is performed by considering a 2D system consisting of 2000 small ABPs with a diameter of σ_s and a mass of m, and one large passive tracer with a diameter of $\sigma_l = 3\sigma_s$ and a mass of M, as sketched in Fig. 1(a). The interactions between the particles are modelled by a repulsive Lennard-Jones-type potential, $U(r) = 4\varepsilon\left[\left(\frac{\sigma}{r}\right)^{24} - \left(\frac{\sigma}{r}\right)^{12}\right] + \varepsilon$, for $r \leq 2^{\frac{1}{12}}\sigma$. The interaction diameter between passive and active particles is taken as $\frac{1}{2}(\sigma_s + \sigma_l)$. The translational motion of the active particles evolves according to the underdamped Langevin equation,

$$m\dot{\mathbf{v}} = -\gamma_s\mathbf{v} + \mathbf{F}_d + \mathbf{F}_r + \boldsymbol{\xi}, \quad (1)$$

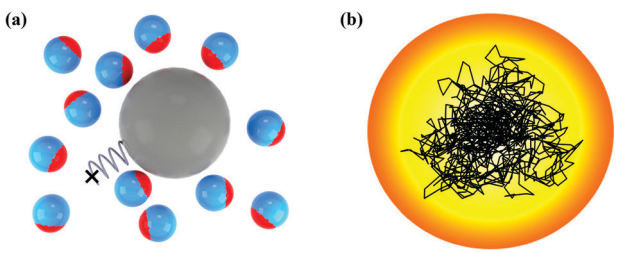

Fig. 1 (a) Schematic diagram of a passive particle (grey) subjected to an external harmonic potential in an active bath consisting of ABPs (Janus). The self-propelling direction of the ABP is marked with the red cap. (b) The motion trajectory of the passive particle in the harmonic trap, which is represented by the colored area.

with $\mathbf{F}_d$ being the self-propulsion force, $\mathbf{F}_r$ being the steric interaction between particles, γ_s being the friction coefficient, and $\boldsymbol{\xi}$ being the Gaussian distributed stochastic force with zero mean and variance $\langle\xi_\alpha(t)\xi_\beta(t')\rangle = 2k_BT\gamma_s\delta_{\alpha\beta}\delta(t-t')$ (α and β represent Cartesian components). In the simulations, we always take $\mathbf{F}_d\sigma_s/k_BT = 20$, which is comparable to the value of the swimming *E. coli* bacteria in experiments. The Brownian rotation of the active particles is similarly simulated with the rotational friction coefficient $\gamma_r = \frac{1}{3}\sigma_s^2\gamma_s$.

The translational motion of the passive particle also follows eqn (1) with the frictional coefficient $\gamma_l = 3\gamma_s$ and $\mathbf{F}_d = 0$. Additionally, the passive tracer is constrained by a harmonic potential $U_{ex}(\mathbf{r}) = \frac{1}{2}k\mathbf{r}^2$, with $\mathbf{r}$ being the tracer displacement from the trap center and k being the trap stiffness. A typical trajectory of the large passive particle trapped in the active bath is plotted in Fig. 1(b). In the simulations, we use the underdamped (instead of overdamped) Langevin equation in order to quantify the kinetic energy of the passive tracer.

Theory

The effect of the active bath on the passive tracer can be theoretically captured by including an active colored noise term in the traditional overdamped Langevin equation,[43–49]

$$\dot{\mathbf{r}} = \mu\mathbf{f}(\mathbf{r}) + \boldsymbol{\eta} + \boldsymbol{\eta}^A, \quad (2)$$

with $\mathbf{f}(\mathbf{r}) = -k\mathbf{r}$ being the restoring force from the external trap, μ being the tracer mobility, $\boldsymbol{\eta}$ being the thermal noise and $\boldsymbol{\eta}^A$ being the active noise. The variance of the thermal noise reads $\langle\eta_\alpha(t)\eta_\beta(t')\rangle = 2D_T\delta_{\alpha\beta}\delta(t-t')$ with D_T being the diffusion coefficient of the passive tracer originating from the thermal bath. The variance of the active noise is $\langle\eta^A_\alpha(t)\eta^A_\beta(t')\rangle = D_A\delta_{\alpha\beta}\exp(-|t-t'|/\tau)/\tau$, where D_A denotes the active contribution to the tracer diffusion coefficient characterizing the strength of the active fluctuations and τ is the correlation time of the active fluctuations. A similar coarse-grained model has been widely used to describe active colloidal particles themselves,[55–60] where $\mathbf{f}(\mathbf{r})$ corresponds to the interactions between the active particles.

In previous work based on eqn (2),[43,45–49] the diffusion coefficient D_T is taken as $D_T = \mu k_BT$, with the mobility μ only originating from the thermal bath. This description does not consider the active friction contributed by the couplings between the tracer and active particles,[49] and is only valid in the dilute limit for active baths.[50] For semidilute or concentrated active particle solutions, μ needs to include both the thermal and active contributions, so that the average friction is balanced by the external force, *i.e.*, $\langle\dot{\mathbf{r}}\rangle/\mu = \langle\mathbf{f}(\mathbf{r})\rangle$ (the friction memory kernel remains instantaneous[44]). In these cases, the thermal diffusion coefficient D_T does not obey the Einstein relation $D_T = \mu k_BT$, since μ now contains the active contributions. In simulations, D_T can be measured as the diffusion coefficient of the tracer in the same active bath when the activities of the constituent swimmers are switched off, such that D_A exclusively corresponds to the active diffusion following its definition.

Following ref. 43, the mean square displacement (MSD) of the passive tracer in the x (or y) direction can be calculated from eqn (2) as

$$\langle \Delta x^2(t) \rangle = \frac{2D_T}{\mu k}\left(1 - e^{-\mu k t}\right) + \frac{2D_A}{\mu k}\frac{1 - e^{-\mu k t} - \mu k \tau\left(1 - e^{-t/\tau}\right)}{1 - (\mu k \tau)^2}. \quad (3)$$

Using eqn (3) to fit the simulation MSD with the independently measured D_T and μ, the strength D_A and the relaxation time τ of the active noise experienced by the passive tracer can be directly extracted.

3 Results and discussion

We first measure the MSD of the passive tracer particle in a semidilute active solution with the packing fraction of the microswimmers $\rho = 0.3$ for various trap stiffness k. Two representative MSD curves with $k\sigma_s^2/k_BT = 40$ and 120 are shown in Fig. 3(a). The MSD data can be well fitted to eqn (3) using D_A and τ as fitting parameters, with $D_T \simeq (0.47 \pm 0.02)k_BT/\gamma_l$ and $\mu \simeq (0.59 \pm 0.01)/\gamma_l$ that are independently measured in simulations. Here, D_T is obtained from the MSD of a passive tracer freely moving in a solution of inactive microswimmers (without activity, $\mathbf{F}_d = 0$), and μ is quantified by the drift velocity of a free passive tracer $\mathbf{v}_d$ under an externally applied force $\mathbf{F}_e$ in the active bath. To properly determine μ, the applied force is so small that the system is in the linear response regime, as demonstrated by the linear relation between $\mathbf{v}_d$ and $\mathbf{F}_e$ in Fig. 2. Note that, in the semidilute situation, the measured D_T and μ significantly deviate from the Einstein relation $D_T = \mu k_BT$, as analyzed in the theory above. For comparison, we also consider a dilute active solution with the microswimmer packing fraction $\rho = 0.06$. The MSD of the passive particle can still be well fitted to eqn (3), as plotted in Fig. 3(c). In this case, the Einstein relation $D_T = k_BT\mu$ is maintained as expected, with $D_T \simeq (0.88 \pm 0.04)k_BT/\gamma_l$ and $\mu \simeq (0.89 \pm 0.01)/\gamma_l$, close to its thermal counterpart.

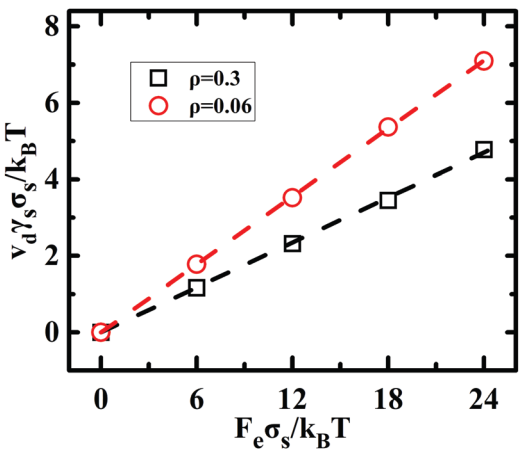

Fig. 2 Reduced drift velocity $\mathbf{v}_d$ of a free passive tracer as a function of externally applied force $\mathbf{F}_e$ in both semi-dilute ($\rho = 0.3$) and dilute ($\rho = 0.06$) active baths. The dahsed line denotes a linear fit to the measured data, with the slope corresponding to μ.

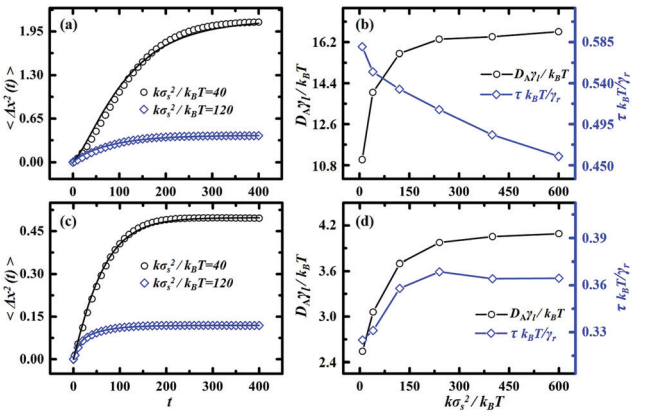

Fig. 3 The MSD in the x direction for various external constraints $k\sigma_s^2/k_BT$ = 40 (black open circles) and $k\sigma_s^2/k_BT$ = 120 (blue open squares) at the packing fractions of the active particles $\rho = 0.3$ (a) and $\rho = 0.06$ (c). Solid lines are fits with eqn (3). The dimensionless D_A (black open circles) and τ (blue open squares) as functions of trap stiffness, extracted by fitting for $\rho = 0.3$ (b) and $\rho = 0.06$ (d).

The quantities D_A and τ obtained from the MSDs show a clear dependence on the trap stiffness k in both semi-dilute and dilute active baths, as plotted in Fig. 3(b) and (d). The strength of the active fluctuations monotonically increases with k for both packing fractions, while the relaxation time of the active noise exhibits a different dependence on k for the semidilute and dilute active baths. The dependence of D_A and τ on the external constraint unambiguously indicates that the active fluctuations experienced by a passive tracer are not an intrinsic property of the active bath, and external constraints must be considered when active noise exists.

The increase of D_A with k can be understood from the collision kinetics between the tracer and the active swimmers. One of the distinctive differences between collisions with passive and active particles is that the momentum change in collisions with passive particles depends only on the momenta before the collision, while additional momentum can be transferred to the tracer from the persistent motion of the self-propelling swimmer. The intensity of the persistent collisions with microswimmers, thus D_A, can be greatly influenced by the constraints imposed on the passive tracer. Briefly, for strong constraints, most of the driving force $\mathbf{F}_d$ is transferred to the tracer, leading to a large D_A; while for weak constraints, the friction on the colliding swimmer (moving with the tracer at a relatively large velocity) offsets part of $\mathbf{F}_d$ and weakens the collision intensity. This picture can be qualitatively formulated by implementing an approximate calculation based on microscopic collision processes. For simplicity, we only consider a head-on collision between the passive and active particles (*i.e.*, the swimmer orientation parallel to the vector connecting the swimmer and tracer). Further, we assume that before the collision, the passive tracer rests at the trap center; and after the collision, the swimmer moves with the tracer for a duration of the orientational relaxation timescale of the

swimmer, $\tau_r = \gamma_r/k_BT$. Disregarding the thermal stochastic force (only considering active collisions), the overdamped Langevin equation of the tracer particle reads $(\gamma_l + \gamma_s)\dot{\mathbf{r}} = -k\mathbf{r} + \mathbf{F}_d$, which is obtained by noticing that $\mathbf{F}_d - \gamma_s\dot{\mathbf{r}}$ corresponds to the force exerted on the tracer by the swimmer. By solving this equation, we obtain the tracer trajectory

$$\mathbf{r}(t) = \frac{\mathbf{F}_d}{k}[1 - \exp(-kt/\gamma)], \quad (4)$$

with $\gamma = \gamma_l + \gamma_s$. The active stochastic force, $\boldsymbol{\eta}^A/\mu$, arising from the persistent collisions between the swimmer and tracer is roughly proportional to $\mathbf{F}_d - \gamma_s\dot{\mathbf{r}}$. Hence, $\langle \boldsymbol{\eta}^A \cdot \boldsymbol{\eta}^A \rangle / \mu^2 \sim \frac{1}{\tau_r}\int_0^{\tau_r} (\mathbf{F}_d - \gamma_s\dot{\mathbf{r}})^2 dt$, which can be evaluated using eqn (4). With the equal-time correlation of the active noise $\langle \boldsymbol{\eta}^A(t)\cdot\boldsymbol{\eta}^A(t)\rangle = 2D_A/\tau$, we obtain $D_A \sim \frac{1}{2}\tau\mu^2\mathbf{F}_d^2\left\{1 - \frac{2\gamma_s}{\tau_r k}[1 - \exp(-\tau_r k/\gamma)] + \frac{\gamma_s^2}{2\gamma\tau_r k}[1 - \exp(-2\tau_r k/\gamma)]\right\}$, which monotonically increases with k and saturates at large k, consistent with the simulation results in Fig. 3. These calculations do not consider the events of the tracer simultaneously colliding with multiple swimmers or the swimmer–tracer collision frequency.

The k dependence of the relaxation time of the active noise can be understood by considering non-head-on collisions between the tracer and the swimmers. For non-head-on collisions in dilute solutions, strong constraints prevent the tracer particle from disengaging from the colliding swimmer, which results in a more persistent collision and hence a longer τ (Fig. 3(d)), and *vice versa*. The decrease of τ in semidilute solutions (Fig. 3(b)), however, is probably due to the accumulation of microswimmers around the passive tracer and the formation of multi-layer structures of swimmers.[61,62] This accumulation effect enhances with increasing the constraint, as active swimmers are more likely to accumulate around an immobile tracer than around a mobile one. Surrounded by layers of active swimmers, the tracer experiences multiple collisions from all directions, decreasing the correlation time of the active noise.

Analogous to the temperature that is related to the magnitude of thermal noise, the effective temperature of the active bath could reflect the strength of active noise to some extent. The concept of effective temperature provides a possible way to map nonequilibrium to equilibrium systems, and it has been often employed to describe active systems based on the well-established equilibrium analyses.[33–37,43,51] So far, we have shown that the active noise is not an intrinsic property of the active bath and is significantly influenced by external potential fields. It is therefore reasonable to expect that the effective temperatures in an active system might be constraint-dependent. In the following, we investigate how external constraints affect the effective temperature of the passive tracer in the active bath. We consider three widely-used definitions of effective temperature, which are separately quantified as the ratio of fluctuation to dissipation $(D_A + D_T)/\mu$, the mean kinetic energy E and the mean potential energy U of the tracer.

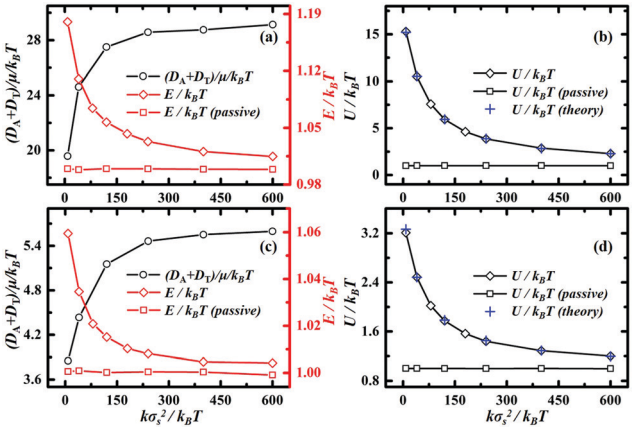

Fig. 4 The effective temperatures defined by the ratio of fluctuation to dissipation $(D_A + D_T)/\mu$ (black open circles, left longitudinal axis) and average kinetic energy E (red open diamonds, right longitudinal axis) as functions of the trap stiffness for $\rho = 0.30$ (a) and $\rho = 0.06$ (c). The effective temperatures defined by average potential energy U as a function of the trap stiffness for $\rho = 0.30$ (b) and $\rho = 0.06$ (d), where the diamonds and crosses correspond to the simulation measurement and theoretical calculation with eqn (5). For comparison, the mean potential and kinetic energies of the tracer in an equilibrium bath are also provided (squares), in which the activities of the microswimmers are turned off.

Fig. 4 plots the measured effective temperatures as a function of trap stiffness in different concentrations of active swimmers. The thermal temperatures in passive thermal baths are also plotted for comparison. All three effective temperatures depend on the stiffness of the external trap, although with different trends. The ratio of the fluctuation to dissipation $(D_A + D_T)/\mu$ is markedly higher than the thermal temperature, and increases with the trap stiffness until saturation at large k. This trend can be qualitatively understood in terms of the k dependence of D_A discussed above, as D_T and μ remain unchanged.

The second effective temperature E is obtained by directly measuring the average kinetic energy of the passive tracer, $\frac{1}{2}M\langle \mathbf{V}^2\rangle$, in underdamped Brownian dynamics simulations. As plotted in Fig. 4(a) and (c), E decreases with the trap stiffness, which is qualitatively opposite to $(D_A + D_T)/\mu$. The E dependence on k, however, is relatively weak, with E only slightly higher than the thermal temperature. The explanation of this trend is straightforward. The tracer obtains additional kinetic energy from collisions with the microswimmers in the active bath. Consider a trapped passive tracer, its mean kinetic energy reads $E = \frac{1}{2}M\left\langle (\mathbf{V}_0 + \mathbf{V}_A)^2\right\rangle = k_BT + \frac{1}{2}M\langle \mathbf{V}_A^2\rangle$, where $\mathbf{V}_0$ and $\mathbf{V}_A$ are the velocities contributed by the thermal bath and the persistent collisions from the active particles, respectively. In the present system, $\mathbf{V}_0$ and $\mathbf{V}_A$ are uncorrelated, and $\mathbf{V}_A \ll \mathbf{V}_0$. The active contribution to the mean kinetic energy, E_A, can be roughly estimated through eqn (4) as $E_A \sim \frac{1}{2}M\langle \mathbf{V}_A^2\rangle \sim \frac{M}{2\tau_r}\int_0^{\tau_r}\dot{\mathbf{r}}^2 dt = \frac{M\mathbf{F}_d^2}{4\tau_r\gamma k}[1 - \exp(-2\tau_r k/\gamma)]$, which monotonically decreases with k and saturates at large k, consistent with the simulation measurement in Fig. 4(a) and (c).

Fig. 4(b) and (d) plot the mean potential energy, U, of the confined passive tracer in active baths of different concentrations, as a function of trap stiffness. Similar to the kinetic energy, the potential energy U also decreases monotonically with k, and remains above k_BT for all the k investigated. The range of U, however, is much greater than that of E. During the collisions between the tracer and the swimmers, the persistent driving force of the swimmer can displace the tracer from the trap center, which results in an additional potential energy for the tracer. Combined with the thermal bath contribution k_BT, the total mean potential energy of the tracer can be approximately calculated from eqn (4) as $U \sim k_BT + \frac{1}{\tau_r}\int_0^{\tau_r}\frac{k}{2}\mathbf{r}^2 dt = k_BT + \frac{\mathbf{F}_d^2}{2k} - \frac{3\mathbf{F}_d^2\gamma}{4\tau_r k^2}\left[1 - \frac{4}{3}\exp(-\tau_r k/\gamma) + \frac{1}{3}\exp(-2\tau_r k/\gamma)\right]$, which decreases with k and saturates at large k, in qualitative agreement with the simulations.

A more quantitative expression of the potential energy can be derived from eqn (3) by taking $t \to \infty$,

$$U = \frac{D_T}{\mu} + \frac{D_A}{\mu}\frac{1}{1+\mu k\tau}. \quad (5)$$

The first term on the right side of eqn (5) is related to the thermal noise contribution that remains constant in a given system. However, D_T/μ generally does not equal k_BT, since μ contains the active friction. The second term depends on the stiffness coefficient not only through k in the denominator, but also through both D_A and τ. The potential energy of the tracer particle can then be determined by eqn (5), using D_T, μ, and k-dependent D_A and τ obtained from simulations. Fig. 4(b) and (d) show that the theoretical values of U (crosses) thus obtained agree perfectly with the measured potential energy in simulations (diamonds). On the other hand, when constant D_A and τ are applied, the predictions of eqn (5) deviate significantly from the measured potential energy (not shown), which further confirms that the active noise experienced by a passive tracer depends sensitively on its external constraint.

4 Conclusion

Active noise provides us with an ideal framework to coarse grain an active bath. Using computer simulations and theoretical calculations, we here show that the active noise experienced by a harmonically trapped passive tracer in an active bath, as well as three related effective temperatures, depends sensitively on the external constraint imposed on the passive particle, which is fundamentally different from the equilibrium cases. This constraint dependence arises from the persistent collisions between the passive tracer and the active swimmers, which can be greatly impacted by the constraint strength. Our results unequivocally demonstrate that the active noise and effective temperatures are not intrinsic properties of active baths, and great care must be taken when applying these quantities in active systems. Our findings are experimentally verifiable by optically trapping a colloidal sphere in a bacterial solution.

Conflicts of interest

There are no conflicts to declare.

Acknowledgements

We acknowledge support from the National Natural Science Foundation of China (Grant No. 11874397, 11874395, 11674365, 11774393 and 11774394) and the K. C. Wong Education Foundation.

References

1 M. C. Marchetti, J. F. Joanny, S. Ramaswamy, T. B. Liverpool, J. Prost, M. Rao and R. A. Simha, *Rev. Mod. Phys.*, 2013, **85**, 1143.
2 J. Elgeti, R. G. Winkler and G. Gompper, *Rep. Prog. Phys.*, 2015, **78**, 056601.
3 C. Bechinger, R. Di Leonardo, H. Löwen, C. Reichhardt, G. Volpe and G. Volpe, *Rev. Mod. Phys.*, 2016, **88**, 045006.
4 H. P. Zhang, A. Be'er, E. L. Florin and H. L. Swinney, *Proc. Natl. Acad. Sci. U. S. A.*, 2010, **107**, 13626.
5 H. Wioland, F. G. Woodhouse, J. Dunkel, J. O. Kessler and R. E. Goldstein, *Phys. Rev. Lett.*, 2013, **110**, 268102.
6 R. D. Leonardo, L. Angelani, D. Dell'Arciprete, G. Ruocco, V. Iebba, S. Schippa, M. Conte, F. Mecarini, F. D. Angelis and E. Di Fabrizio, *Proc. Natl. Acad. Sci. U. S. A.*, 2010, **107**, 9541.
7 H.-R. Jiang, N. Yoshinaga and M. Sano, *Phys. Rev. Lett.*, 2010, **105**, 268302.
8 J. Palacci, S. Sacanna, A. P. Steinberg, D. J. Pine and P. M. Chaikin, *Science*, 2013, **339**, 936.
9 W. F. Paxton, K. C. Kistler, C. C. Olmeda, A. Sen, S. K. Angelo, Y. Cao, T. E. Mallouk, P. E. Lammert and V. H. Crespi, *J. Am. Chem. Soc.*, 2004, **126**, 13424.
10 I. Theurkauff, C. Cottin-bizonne, J. Palacci, C. Ybert and L. Bocquet, *Phys. Rev. Lett.*, 2012, **108**, 268303.
11 A. Sokolov and I. S. Aranson, *Phys. Rev. Lett.*, 2012, **109**, 248109.
12 A. Sokolov, I. S. Aranson, J. O. Kessler and R. E. Goldstein, *Phys. Rev. Lett.*, 2007, **98**, 158102.
13 K. K. Dey, X. Zhao, B. M. Tansi, W. J. Méndez-Ortiz, U. M. Córdova-Figueroa, R. Golestanian and A. Sen, *Nano Lett.*, 2015, **15**, 8311.
14 A. Kaiser and H. Löwen, *J. Chem. Phys.*, 2014, **141**, 044903.
15 J. Harder, C. Valeriani and A. Cacciuto, *Phys. Rev. E: Stat., Nonlinear, Soft Matter Phys.*, 2014, **90**, 062312.
16 M. Paoluzzi, R. Di Leonardo, M. C. Marchetti and L. Angelani, *Sci. Rep.*, 2016, **6**, 34146.
17 N. Nikola, A. P. Solon, Y. Kafri, M. Kardar, J. Tailleur and R. Voituriez, *Phys. Rev. Lett.*, 2016, **117**, 098001.
18 G. Junot, G. Briand, R. Ledesma-Alonso and O. Dauchot, *Phys. Rev. Lett.*, 2017, **119**, 028002.
19 C. Wang, Y.-K. Guo, W.-D. Tian and K. Chen, *J. Chem. Phys.*, 2019, **150**, 044907.

20 L. Angelani, C. Maggi, M. L. Bernardini, A. Rizzo and R. Di Leonardo, *Phys. Rev. Lett.*, 2011, **107**, 138302.
21 D. Ray, C. Reichhardt and C. J. O. Reichhardt, *Phys. Rev. E: Stat., Nonlinear, Soft Matter Phys.*, 2014, **90**, 013019.
22 R. Ni, M. A. Cohen Stuart and P. G. Bolhuis, *Phys. Rev. Lett.*, 2015, **114**, 018302.
23 W. Gao, A. Pei, X. Feng, C. Hennessy and J. Wang, *J. Am. Chem. Soc.*, 2013, **135**, 998.
24 P. Dolai, A. Simha and S. Mishra, *Soft Matter*, 2018, **14**, 6137.
25 L. Angelani, *J. Phys.: Condens. Matter*, 2019, **31**, 075101.
26 S. C. Takatori and J. F. Brady, *Soft Matter*, 2015, **11**, 7920.
27 J. Stenhammar, R. Wittkowski, D. Marenduzzo and M. E. Cates, *Phys. Rev. Lett.*, 2015, **114**, 018301.
28 X.-L. Wu and A. Libchaber, *Phys. Rev. Lett.*, 2000, **84**, 3017.
29 Y. Peng, L. Lai, Y.-S. Tai, K. Zhang, X. Xu and X. Cheng, *Phys. Rev. Lett.*, 2016, **116**, 068303.
30 L. Angelani, R. Di Leonardo and G. Ruocco, *Phys. Rev. Lett.*, 2009, **102**, 048104.
31 A. Sokolov, M. M. Apodaca, B. A. Grzybowski and I. S. Aranson, *Proc. Natl. Acad. Sci. U. S. A.*, 2010, **107**, 969.
32 S. A. Mallory, C. Valeriani and A. Cacciuto, *Phys. Rev. E: Stat., Nonlinear, Soft Matter Phys.*, 2014, **90**, 032309.
33 D. Loi, S. Mossa and L. F. Cugliandolo, *Phys. Rev. E: Stat., Nonlinear, Soft Matter Phys.*, 2008, **77**, 051111.
34 D. Loi, S. Mossa and L. F. Cugliandolo, *Soft Matter*, 2011, **7**, 3726.
35 G. Szamel, *Phys. Rev. E: Stat., Nonlinear, Soft Matter Phys.*, 2014, **90**, 012111.
36 J. Palacci, C. Cottin-Bizonne, C. Ybert and L. Bocquet, *Phys. Rev. Lett.*, 2010, **105**, 088304.
37 F. Ginot, I. Theurkauff, D. Levis, C. Ybert, L. Bocquet, L. Berthier and C. Cottin-Bizonne, *Phys. Rev. X*, 2015, **5**, 011004.
38 S. C. Takatori, W. Yan and J. F. Brady, *Phys. Rev. Lett.*, 2014, **113**, 028103.
39 T. Speck, *EPL*, 2016, **114**, 30006.
40 É. Fodor, C. Nardini, M. E. Cates, J. Tailleur, P. Visco and F. van Wijland, *Phys. Rev. Lett.*, 2016, **117**, 038103.
41 D. Mandal, K. Klymko and M. R. DeWeese, *Phys. Rev. Lett.*, 2017, **119**, 258001.
42 E. Frey and K. Kroy, *Ann. Phys.*, 2005, **14**, 20.
43 C. Maggi, M. Paoluzzi, N. Pellicciotta, A. Lepore, L. Angelani and R. Di Leonardo, *Phys. Rev. Lett.*, 2014, **113**, 238303.
44 C. Maggi, M. Paoluzzi, L. Angelani and R. Di Leonardo, *Sci. Rep.*, 2017, **7**, 17588.
45 A. Argun, A.-R. Moradi, E. Pinçe, G. B. Bagci, A. Imparato and G. Volpe, *Phys. Rev. E*, 2016, **94**, 062150.
46 S. Chaki and R. Chakrabarti, *Physica A*, 2018, **511**, 302.
47 S. Chaki and R. Chakrabarti, *Physica A*, 2019, **530**, 121574.
48 K. Goswami, *Phys. Rev. E*, 2019, **99**, 012112.
49 L. Dabelow, S. Bo and R. Eichhorn, *Phys. Rev. X*, 2019, **9**, 021009.
50 D. T. Chen, A. Lau, L. A. Hough, M. F. Islam, M. Goulian, T. C. Lubensky and A. G. Yodh, *Phys. Rev. Lett.*, 2007, **99**, 148302.
51 S. Krishnamurthy, S. Ghosh, D. Chatterji, R. Ganapathy and A. K. Sood, *Nat. Phys.*, 2016, **12**, 1134.
52 U. Seifert, *Rep. Prog. Phys.*, 2012, **75**, 126001.
53 A. P. Solon, Y. Fily, A. Baskaran, M. E. Cates, Y. Kafri, M. Kardar and J. Tailleur, *Nat. Phys.*, 2015, **11**, 673.
54 P. Liu, S. Ye, F. Ye, K. Chen and M. Yang, *Phys. Rev. Lett.*, 2020, **124**, 158001.
55 L. Caprini, U. M. B. Marconi and A. Puglisi, *Sci. Rep.*, 2019, **9**, 1386.
56 U. M. B. Marconi and C. Maggi, *Soft Matter*, 2015, **11**, 8768.
57 S. Shankar and M. C. Marchetti, *Phys. Rev. E*, 2018, **98**, 020604.
58 A. Puglisi and U. Marini Bettolo Marconi, *Entropy*, 2017, **19**, 356.
59 C. Sandford, A. Y. Grosberg and J.-F. Joanny, *Phys. Rev. E*, 2017, **96**, 052605.
60 G. Szamel, *EPL*, 2017, **117**, 50010.
61 T. Jamali and A. Naji, *Soft Matter*, 2018, **14**, 4820.
62 J. Elgeti and G. Gompper, *EPL*, 2013, **101**, 48003.

